Poly(triacetylene) Oligomers: Synthesis, Characterization, and Estimation of the Effective Conjugation Length by Electrochemical, UV/Vis, and Nonlinear Optical Methods

Rainer E. Martin, Ulrich Gubler, Corinne Boudon, Volker Gramlich, Christian Bosshard, Jean-Paul Gisselbrecht, Peter Günter, Maurice Gross, and François Diederich*

Dedicated to Professor Dieter Seebach on the occasion of his 60th birthday

Abstract: Poly(triacetylene)s [PTAs, $-(C\equiv C-CR=CR-C\equiv C)_n-$] are a new class of linearly conjugated polymers with a nonaromatic all-carbon backbone. To explore structure–property relationships in PTAs, we prepared a series of monodisperse oligomers ranging from monomer to hexamer by oxidative Glaser–Hay coupling of a bifunctional ("chain-forming") (*E*)-hex-3-ene-1,5-diyne in the presence of an endcapping unit. All six oligomers are amazingly stable towards exposure to light, air, and temperatures beyond their melting points. They have been fully characterized and are readily soluble in a wide range of solvents. The conjugated rods are reversibly reduced in one-electron transfer steps and cannot be oxidized below +1.23 V vs. Fc/Fc^+. The effective conjugation length in PTAs was estimated from the electronic absorption (UV/Vis) data, and various evaluation methods yielded convergence of the optical properties in the range of 7 to 10 monomer units. The nonresonant second-order molecular hyperpolarizability γ was measured in $CHCl_3$ by means of the third harmonic generation (THG) at $\lambda = 1.907$ μm. A plot of γ/n vs. n revealed a power law $\gamma \approx n^a$ for γ with a fitted exponent $a = 2.5 \pm 0.1$. From the THG measurements, an effective conjugation length of about 10 monomer units was found, in surprisingly good agreement with the value obtained from UV/Vis spectroscopy data.

Keywords
conjugation length · electrochemistry · nonlinear optics · oligomers · poly(triacetylene)s

Introduction

An increasing number of conjugated organic materials and polymers are widely explored as advanced materials for electronic and photonic applications,[1] since they possess inherent synthetic flexibility, potential ease of processing, and the possibility of tailoring material characteristics to suit a desired property. Conjugated organic molecules of multinanometer length are of particular interest for use as molecular wires with potential application in the emerging field of molecular electronics.[2] Oligomers of defined length also play an important role for establishing structure–property relationships in the corresponding long-chain conjugated polymers.[3]

The number of repeat units in a conjugated polymer required to furnish size-independent redox, optical, or other properties is of great general interest. Although the effective π-electron delocalization length cannot be measured directly, the idea of "conjugation length" or "effective conjugation length" has become one of the central concepts in the theoretical and experimental understanding of many properties of conjugated polymers.[4a] The usefulness of monodisperse oligomers for the experimental determination of the effective conjugation length has been widely demonstrated.[4]

We recently reported poly(triacetylene)s [PTAs, $-(C\equiv C-CR=CR-C\equiv C)_n-$][5, 6] as the third linearly conjugated polymers with a nonaromatic all-carbon backbone in the progression which starts with polyacetylene [$-(CR=CR)_n-$; PA] and poly(diacetylene) [$-(C\equiv C-CR=CR)_n-$; PDA], and ultimately leads to carbyne [$-(C\equiv C)_n-$]. To explore structure–property relationships in PTAs, we had also prepared a series of stable monodisperse oligomers ranging from phenylacetylene endcapped monomer **1a** to pentamer **1e**.[7] Although trends in electrochemical[8] and linear optical properties in this series have been investigated, difficulties in large-scale preparation and poor solubility prevented a more extensive investigation of the physical properties of these molecular rods as a function of their length.

[*] Prof. F. Diederich, Rainer E. Martin
Laboratorium für Organische Chemie, ETH-Zentrum
Universitätstrasse 16, CH-8092 Zürich (Switzerland)
Fax: Int. code +(1)632-1109
Prof. P. Günter, Dr. C. Bosshard, U. Gubler
Institut für Quantenelektronik
ETH-Hönggerberg, CH-8093 Zürich (Switzerland)
Prof. Dr. V. Gramlich
Institut für Kristallographie und Petrographie, ETH-Zentrum
Sonneggstrasse 5, CH-8092 Zürich (Switzerland)
Prof. M. Gross, Dr. C. Boudon, Dr. J.-P. Gisselbrecht
Laboratoire d'Electrochimie et de Chimie Physique du Corps Solide,
Faculté de Chimie, Université Louis Pasteur
1 et 4, rue Blaise Pascal, B: P. 296, F-67008 Strasbourg Cedex (France)

  0947-6539/97/0309-1505 $ 17.50+.50/0

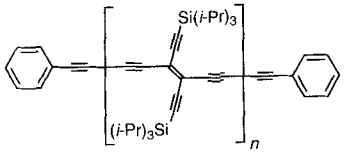

	n
1a	1
1b	2
1c	3
1d	4
1e	5

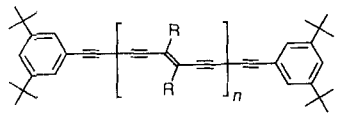

	R	X_n	M_n
2	C≡C–Si(*i*-Pr)$_3$	22	9600
3a	$CH_2OSitert\text{-}BuMe_2$	31	11300
3b	$CH_2OSitert\text{-}BuMe_2$	22	8000

To determine the effective conjugation length in PTAs, we prepared a new, much more soluble and readily available series of monodisperse PTA oligomers ranging from monomer **4a**[5, 9] to hexamer **4f**. Here, we examine the trends in electrochemical (cyclic voltammetry), linear optical (UV/Vis), and nonlinear optical (third harmonic generation) properties within this series and compare our results to those previously described for oligomeric (**1a–e**) and polydisperse longer-chain PTAs (**2**, **3a**, and **3b**).[5] By use of various evaluation methods, estimations of the effective conjugation length in poly(triacetylene) polymers are made.

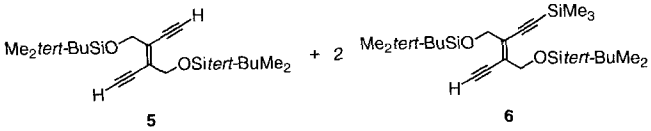

	n	yield
4b	2	58%
4c	3	20%
4d	4	9%
4e	5	2%
4f	6	1%

Scheme 1. a) CuCl, TMEDA, CH_2Cl_2, molecular sieves 4 Å, O_2, 20 °C, 2 h. TMEDA = *N*,*N*,*N*′,*N*′-tetramethylenediamine.

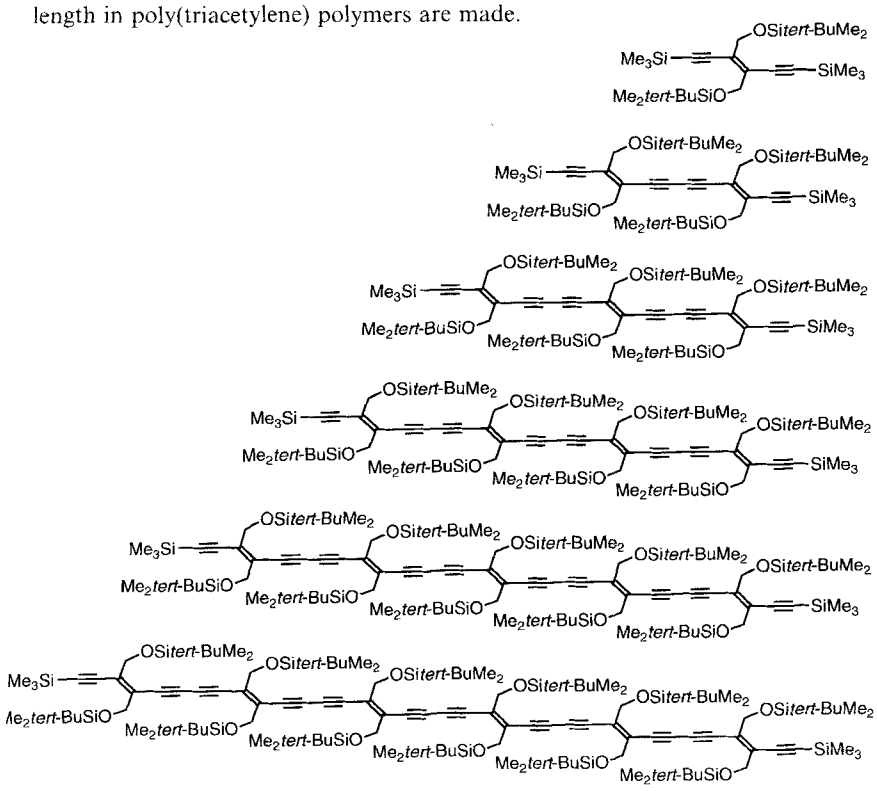

Results and Discussion

Synthesis and Structural Characterization: The synthesis of oligomers **4b–f** by oxidative Glaser–Hay polymerization of (*E*)-hex-3-ene-1,5-diyne (**5**)[5, 9] in the presence of **6**,[9a] bearing the endcapping Me_3Si group, was carried out in dry CH_2Cl_2 at room temperature (Scheme 1). The size distribution of the oligomers was strongly dependent on the reaction conditions and the ratio of the two starting materials. The individual oligomers **4b–f** were isolated by a combination of size-exclusion chromatography (CH_2Cl_2, Bio-Beads S-X1 beads), flash chromatography (SiO_2, hexane/PhMe 1:1), and precipitation from MeOH. Higher oligomers were also formed, but were not separable despite their good solubility. All compounds are stable towards exposure to light, air, and temperatures beyond their melting points and are readily soluble in a wide range of solvents (Table 1).

The number of monomer units in **4a–f** was confirmed by means of their ^1H and ^{13}C NMR spectra, which show n sp^2 and $2n$ sp carbon atom resonances, where n is the number of monomer units. In the ^{13}C NMR spectra of **4a–f**, all sp^2 and sp carbon atom resonances are clearly separated, and coalescence of peaks begins only at the stage of the hexamer. The resonances of the terminal double bonds in **4c–f** appear around $\delta = 129.5$ and 133.5 and those of the interior alkene moieties near $\delta = 132$. Correspondingly, the sp^2 carbon atoms in the polydisperse polymers **3a** and **3b** give a single peak at $\delta = 132.37$.[5] In accord with studies on poly(enyne)s and related systems,[10] we did not find the ^{13}C NMR data very useful for estimating the effective conjugation length of our PTA materials.

The rigid rodlike oligomers are between 9.6 Å (**4a**) and 46.1 Å (**4f**) in length (measured from terminal Si to Si), as shown by force-field energy-minimization calculations (Table 1).[11] A general formula for estimating the oligomeric length (l) is given by l (Å) $= 7.3(n-1) + 9.6$, where n is the number of monomeric subunits. The computed length for monomer **4a** is in good agreement with the value found by X-ray structural analysis, which shows a distance between the two Si atoms at the termini of 9.71 Å (Figure 1, top). Similarly to **4a**, the free diethynyl derivative **5** has a nearly perfectly planar carbon framework in its X-ray crystal structure, with a maximum deviation from the least-squares plane passing through the entire conjugated carbon backbone of only 0.02 Å (Figure 1, bottom).

0947-6539/97/0309-1506 $ 17.50+.50/0 *Chem. Eur. J.* **1997**, *3*, No. 9

Table 1. Physical and optical properties of oligomers **4a–f**.

	n	l [Å] [a]	M.p. [°C] [b]	λ_{em} [nm] [c]	λ_{max} [nm] (eV) [d]	ε [$M^{-1}cm^{-1}$] [e]	E_g [eV] (nm) [f]
4a	1	9.6	49	–	296.4±0.1 (4.18)	19700	4.01 (309)
4b	2	16.9	97	425	378.1±0.1 (3.28)	24200	3.14 (395)
4c	3	24.2	138	445	420.3±0.1 (2.95)	28600	2.82 (439)
4d	4	31.5	168	–	439.0±0.2 (2.82)	35200	2.67 (464)
4e	5	38.8	189	–	458.9±0.4 (2.70)	29700	2.58 (480)
4f	6	46.1	196	–	463.6±0.5 (2.67)	36500	2.54 (488)

[a] Length estimated by energy minimization calculations [11]. [b] Uncorrected. [c] Longest-wavelength emission in $CHCl_3$, λ_{ex} = 300 nm. [d] Longest-wavelength absorption in $CHCl_3$ at room temperature, obtained by deconvolution of the absorption spectra. [e] Molar extinction coefficient. [f] Solution optical gap.

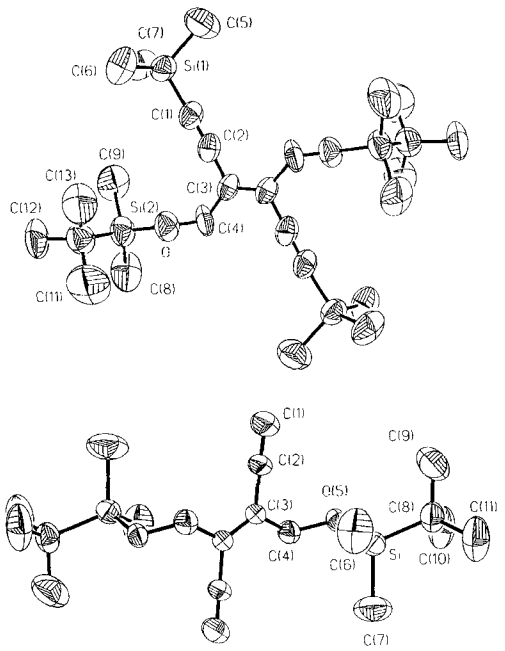

Figure 1. Molecular structures in the crystals of **4a** (top) and **5** (bottom). Selected bond lengths [Å] and angles [°] in **5**: C(1)–C(2) 1.162(6), C(2)–C(3) 1.425(5), C(3)–C(3A) 1.349(7), C(3)–C(4) 1.511(5), C(4)–O(5) 1.423(5), Si–O(5) 1.649(3); C(1)-C(2)-C(3) 176.3(5), C(2)-C(3)-C(4) 115.6(3), C(4)-C(3)-C(3A) 123.0(4), C(3)-C(4)-O(5) 111.9(3), Si-O(5)-C(4) 125.7(2).

Electrochemistry: The electrochemical properties of **4a–f** were examined by steady-state voltammetry, polarography, and cyclic voltammetry (Table 2) in THF or CH_2Cl_2 with 0.1 M Bu_4NPF_6 as the supporting electrolyte. Whereas all six conjugated rods were reversibly reduced in one-electron transfer steps, they could not be oxidized below +1.23 V vs. Fc/Fc^+. This result helps to explain their amazing stability to laboratory air over periods of months. With increasing oligomeric length, the first reversible reduction step became increasingly facile. A comparison between **4a–f** with the corresponding oligomers in the series **1a–e**,[7, 8] however, clearly showed that the reduction of the former requires much more negative potentials in each case. At the stage of the oligomers, the pendant alkynyl groups and the phenylacetylene endcapping groups in **1a–e** provide a significantly larger stabilization of the lowest unoccupied molecular orbital (LUMO) than the pendant $Me_2tBuSiOCH_2$ groups and the Me_3Si endcapping residues in **4a–f**. Comparisons between **1b–c** and the corresponding oligomers with $(iPr)_3Si$ instead of PhC≡C endcapping groups showed that the influence of these groups on the first reduction potential rapidly decreases with oligomeric length: the first reduction potentials vs. Fc/Fc^+ in THF (+0.1 M Bu_4NPF_6) for the $(iPr)_3Si$-endcapped oligomers corresponding to **1b,c** are −1.52 (dimer) and −1.23 V (trimer).[7b, 8]

Table 2. Cyclic voltammetric reduction characteristics of oligomers **1a–e** [7,8] and **4a–f**.

	E'°(red.) [a]		E'°(red. 1) [b]	E_{pc}(red. 2) [c]	E_{pa}(ox.) [d]
1a	−1.57	**4a**	−2.68 [a]	–	–
1b	−1.32, −1.60	**4b**	−2.10	–	1.29
1c	−1.17, −1.42, −2.00	**4c**	−1.88	−2.09	1.25
1d	−1.14, −1.32, −1.76, −1.99	**4d**	−1.80	−1.95	1.23
1e	−1.07, −1.24, −1.55, −1.65, −1.85	**4e**	−1.75	−2.30	1.23
		4f	−1.71	−2.30	1.23

[a] V vs. Fc/Fc^+, Hg electrodes in THF +0.1 M Bu_4NPF_6, formal redox potential $E'^\circ = (E_{pa}+E_{pc})/2$. [b] V vs. Fc/Fc^+, glassy carbon electrode in CH_2Cl_2 + 0.1 M Bu_4NPF_6, formal redox potential $E'^\circ = (E_{pa}+E_{pc})/2$. [c] Peak potential E_{pc} for irreversible reduction. [d] Peak potential E_{pa} for irreversible oxidation.

The second striking difference between the two sets of oligomers is that the number of reversible one-electron reduction steps for **1a–e** corresponds directly to the number of tetraethynylethene (TEE) moieties in each rod, whereas in the series **4a–f**, only a second, irreversible reduction step is observed for trimer to hexamer.

The disparity in the first reduction potential between the two oligomeric series, however, vanishes upon passing to longer-chain polymers. From small amplitude waves, due to the low solubility of the long-chain PTAs in THF and due to low diffusion coefficients, the first reduction potential have been determined as −0.70 V for **2** and as −0.65 V for **3a**.[5] The shorter 22-mer sample **3b** ($M_w/M_n \approx 2$) was reduced at −0.60 V vs. Fc/Fc^+ on a Hg electrode in CH_2Cl_2 (+ 0.1 M Bu_4NPF_6); this verified nicely the previous results found for **3a**. Figure 2 shows a plot of the first reversible reduction potential versus the number of monomeric units n (top) and as a function of $1/n$ (bottom) for both sets of oligomers as well as for the longer-chain polymers **2**, **3a**, and **3b**. Despite the differences encountered at the stage of the shorter oligomers, the first reduction potentials of both series ultimately converge to the same limiting value at the stage of the longer-chain polymers around −0.6 V. Apparently, the nature of the pendant groups ($(iPr)_3Si-C\equiv C$ vs. $Me_2tBuSiOCH_2$) affects the reduction potentials of PTAs only in the shorter oligomers, whereas the conjugation pathway along the linear all-carbon backbone largely determines the LUMO energy and reducibility in the longer-chain polymers. A linear fit between $1/n$ and the first reduction potential can only be obtained for the shorter oligomer series **1a–e** and **4a–f** (Figure 2, bottom). Upon inclusion of the data for the three polydisperse compounds **2**, **3a**, and **3b**, however, a linear correlation is no longer obtained. In view of the lacking data for intermediate-sized oligomers with $n = 7–20$, an estimation of the effective conjugation length from the electrochemical data is not straightforward.

Electronic Absorption Spectroscopy: The UV/Vis spectra of the series **4a–f** only display a clear longest-wavelength transition λ_{max} for monomer and dimer, whereas for the longer oligomers the lowest-energy transition is covered under a broad, intense

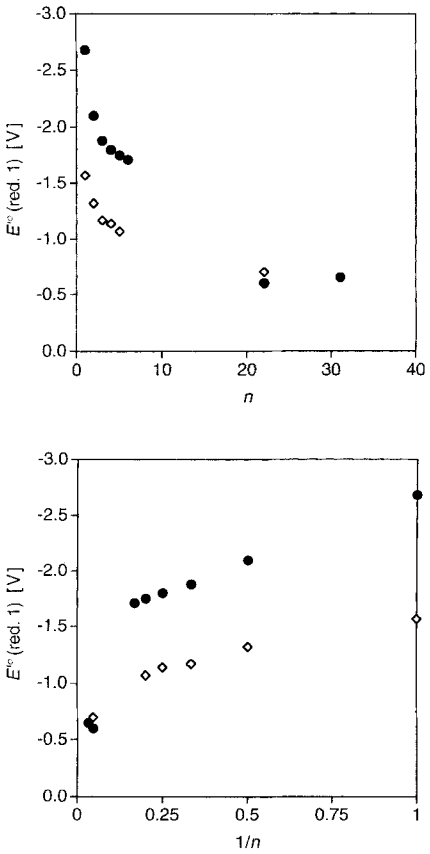

Figure 2. First reduction potentials of **1a–e**, **4a**, **2**, and **3a** in THF (+0.1 M Bu_4NPF_6, V vs. Fc/Fc^+) and of **3b** and **4b f** in CH_2Cl_2 plotted as a function of n (top) and of $1/n$ (bottom). ◇ **1a–e**, **2**; ● **4a–f**, **3a,b**.

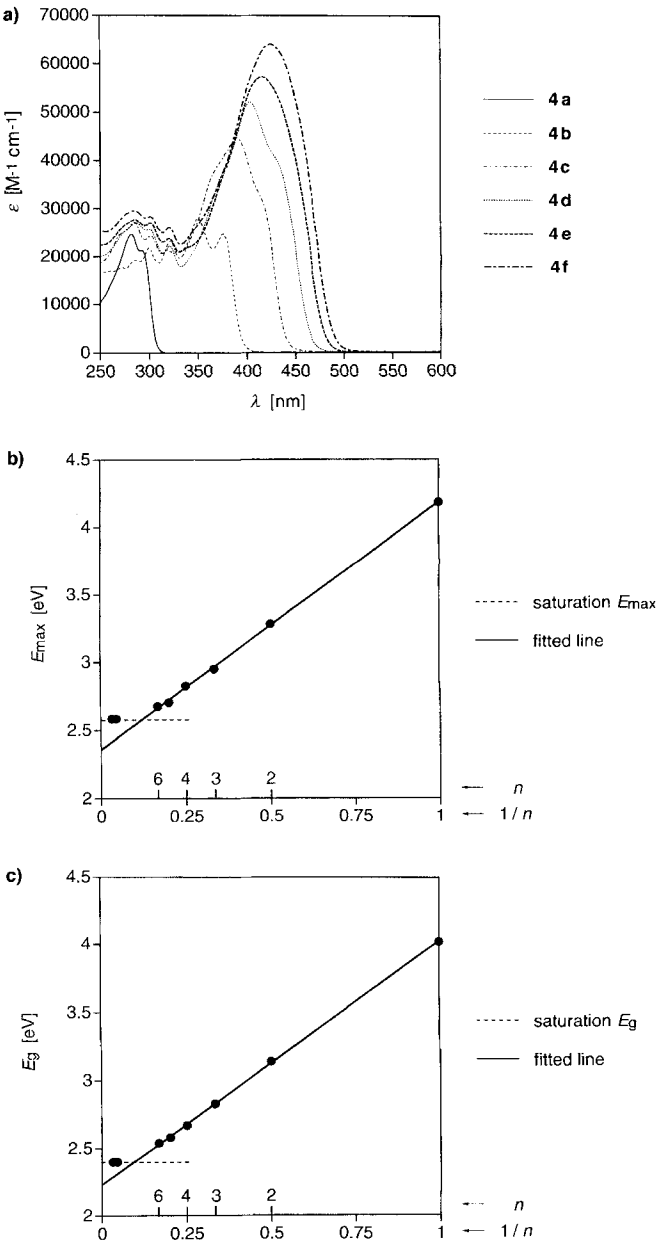

Figure 3. a) Electronic absorption spectra of oligomers **4a–f** in $CHCl_3$. b) Plot of the lowest-energy transition E_{max} vs. $1/n$ (n = number of monomeric units) for the series **4a–f**, **3a**, and **3b**. Linear regression for **4a–f** affords E_{max}(eV) = 1.83(1/n) + 2.35. c) Plot of the solution optical gap energy E_g vs. $1/n$ for the series **4a–f**, **3a**, and **3b**. Linear regression for **4a–f** affords E_g(eV) = 1.78(1/n) + 2.23. In both cases, saturation is observed for **3a** and **3b**, as indicated by the horizontal line. The effective conjugation length is evaluated at the crossing point of both lines.

absorption band. A precise determination of λ_{max} and E_{max}, respectively, therefore required the deconvolution of the UV/Vis spectra. By assuming a sum of Gaussian line shapes in energy space, all spectra could be exactly reproduced. The obtained absorption energies E_{max} and their uncertainties were transformed back to wavelengths and are given in Table 1 for oligomers **4a–f**.[12] With increasing oligomeric length, the longest-wavelength absorptions λ_{max} as well as the end absorptions are increasingly bathochromically shifted. However, no apparent saturation for λ_{max} is reached. In the spectrum of hexamer **4f** (Figure 3a) the lowest-energy transition is fully covered under the broad absorption band. λ_{max} was calculated as 463.6±0.5 nm (E_{max} = 2.67 eV), and the solution optical gap E_g was determined to be 2.54 eV (488 nm).[13] The observation of significant vibrational fine-structure in the spectrum even at the stage of the hexamer provides support for a rigid planar conjugated backbone in solution. Temperature-dependent UV/Vis measurements in n-hexane for pentamer **4e** between 54 and −45 °C gave similar spectra with a weak bathochromic shift of the most intense absorption band from 407 nm at 54 °C to 415 nm at −45 °C. This demonstrates that the conjugation length in PTAs is only slightly affected within this temperature range. Similar findings had been reported for poly(enyne)s serving as model compounds for PDAs.[10] Oligomers **4b** and **4c** displayed a bright fluorescence in $CHCl_3$ solutions (Table 1).

The plot of the most intense absorption band against the reciprocal number of monomer units $1/n$ gave a straight line with an intercept at 445±4 nm (2.79±0.03 eV). This extrapolated value of λ_{max} for the related infinite-chain polymer is in very good agreement with the experimental numbers measured for **3a** (449 nm, 2.76 eV) and **3b** (448 nm, 2.77 eV), demonstrating that **4a–f** are suitable model oligomers for long-chain PTAs. To estimate the effective conjugation length in PTAs, the lowest transition energies E_{max} were plotted as a function of $1/n$ for compounds **4a–f** and **3a-b** (Table 1, Figure 3b).[12] The crossing of the straight line for the oligomers with the horizontal saturation level line for the polymers revealed that the effective conjugation length was reached in PTAs containing 8±1 monomer units, which corresponds to a total of 21–27 double

0947-6539/97/0309-1508 $ 17.50+.50/0 Chem. Eur. J. 1997, 3, No. 9

and triple bonds and a rod length of 53–68 Å. In an analogous evaluation, using the solution optical band gap E_g, a slightly higher value of 10 ± 1 monomer units was obtained (Figure 3c).[14]

To evaluate the effective conjugation length, we also applied a linear expression [Eq. (1)],[15] derived on the basis of the free electron gas model of Kuhn.[16] In Equation (1), E is the

$$E = V_0 + \left(\frac{h^2}{4mL_0^2} - \frac{V_0}{4}\right)\frac{1}{N+0.5} \quad (1)$$

optical absorption energy or band gap, N the number of conjugated double and triple bonds per molecule, V_0 the amplitude of a sinusoidal potential which corrects the free electron gas model for bond length alternation, L_0 the length of the unit of conjugation, h the Planck constant, and m the mass of the electron. Linear regression analysis[10, 15] of the plot of the energy at the longest-wavelength absorption maximum E_{max} against $1/(N+0.5)$ yielded $V_0 = 2.28\pm0.02$ eV and $n = 7\pm1$. Thus, this analysis provided a slightly lower value for n than the analysis of the plot of E_{max} vs. $1/n$ (Figure 3b). A plot of the solution optical band gap E_g vs. $1/(N+0.5)$ gave similar values with $n = 9\pm1$ and $V_0 = 2.16\pm0.02$ eV. Overall, the value for V_0 in PTAs fits very nicely into the general trend seen in the series of PAs ($V_0 = 1.75$ eV), PDAs ($V_0 = 2.25$ eV), and polyyne models of carbyne ($V_0 = 2.50$ eV).[10] In conclusion, this UV/Vis study disclosed that the convergence of the linear optical properties in PTAs is reached in the range of about 7–10 monomer units. In comparison, for PDAs, an effective conjugation length of $n \approx 6$[15] and $n \approx 10$[10] monomer units has been reported, corresponding to 12 or 20 double and triple bonds, respectively, depending on the method of extrapolation.

Third Harmonic Generation: The nonresonant second-order hyperpolarizability γ, measured by means of the third harmonic generation (THG) in $CHCl_3$ solutions at $\lambda = 1.907$ μm[17] was analyzed in the series **4a–f** as a function of oligomeric length (Table 3). For comparison, γ was also determined for the soluble, shorter tetraethynylethene oligomers **1a–c**, in order to estimate the impact of the additional conjugation paths in these molecules, involving the laterally pendant alkyne groups and the additional PhC≡C endcapping groups. From the obtained microscopic hyperpolarizability γ, we estimated a macroscopic hyperpolarizability $\chi^{(3)}$ by assuming an isotropic arrangement of the molecules and using the density and refractive indices (for local field corrections) of the solvent $CHCl_3$. This estimate gives a lower limit of what can be expected in the bulk.

Table 3. Second-order hyperpolarizability of oligomers **1a–c** and **4a–f** from third harmonic experiments at $\lambda = 1.907$ μm. $\chi^{(3)}$ was measured relative to fused silica (fs, 3.9×10^{-22} m^{2}V^{-2} (2.8×10^{-14} esu)).

	n	γ [a] [10^{-36} esu]	γ [a] [10^{-48} m^{5}V^{-2}]	$\frac{\chi^{(3)}_{100}}{\chi^{(3)}_{fs}}$ [b]	$\chi^{(3)}_{100}$ [b] [10^{-12} esu]	$\chi^{(3)}_{100}$ [b] [10^{-20} m^{2}V^{-2}]
1a	1	240	3.41	41	1.1	1.6
1b	2	1030	14.5	105	2.9	4.1
1c	3	2570	35.9	183	5.1	7.2
4a	1	22	0.32	5	0.14	0.19
4b	2	108	1.51	13	0.37	0.52
4c	3	363	5.08	31	0.86	1.2
4d	4	740	10.3	49	1.4	1.9
4e	5	1320	18.5	72	2.0	2.8
4f	6	1780	24.9	79	2.2	3.1

[a] Rotational average of the γ tensor. [b] $\chi^{(3)}$ values are extrapolated from measured values of γ, assuming a linear dependence on concentration. The estimations present a lower limit, since density and the small (with respect to the pure compounds) refractive indices for local field corrections of $CHCl_3$ were used in the calculation of $\chi^{(3)}$.

Different mathematical approaches, such as Hückel-type tight-binding modeling, ab initio calculations, or Pariser–Parr–Pople simulations, predict for conjugated molecules shorter than the critical conjugation length a power law dependence $\gamma \approx n^a$, where n corresponds to the total number of monomer units. For the exponent a, values between 3 and 6 have been reported, depending on the model used.[18] Above the critical conjugation length, the cubic hyperpolarizability γ should saturate and increase only linearly with the number of monomer units n. The related macroscopic susceptibility $\chi^{(3)}$ should not be further enhanced and stay constant.

For the PTA samples **4a–f**, a plot of γ/n vs. n revealed a power law for γ with a fitted exponent $a = 2.5\pm0.1$ (Figure 4).

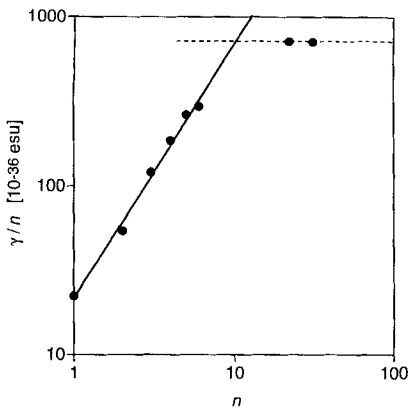

Figure 4. Dependence on conjugation length of the second-order hyperpolarizability γ, presented in a double logarithmic plot of γ/n vs. n. For oligomers **4a–f**, a power law $\gamma \approx n^a$ ($a = 2.5\pm0.1$) is obtained (solid line), and for the polydisperse polymers **3a** and **3b**, saturation (broken line). The effective conjugation length is evaluated at the crossing point of both lines.

THG measurements of a polydisperse film sample of **3a**[5] showed a macroscopic susceptibility $\chi^{(3)} = 7.8\times10^{-20}$ m^{2}V^{-2} (5.6×10^{-12} esu), and in solution this value was reproduced for **3b** within one percent, confirming that the limit of the critical conjugation length is certainly passed. The corresponding γ/n values for **3a** ($\gamma = 300\times10^{-48}$ m^{5}V^{-2}, 22000×10^{-36} esu) and **3b** ($\gamma = 219\times10^{-48}$ m^{5}V^{-2}, 15650×10^{-36} esu) are included in Figure 4, and the saturation level is indicated by a horizontal line. The crossing of the power law and the saturation level yields a critical conjugation length of about 10 monomer units (30 double and triple bonds), in good agreement with the value obtained from UV/Vis spectroscopy. It is not yet clearly understood whether linear absorption and second-order hyperpolarizability data should lead to the same critical conjugation length, but it seems to hold true in the case of PTAs.

Only few nonlinear optical data as a function of chain length have been reported for linearly conjugated polymers, owing to the often difficult synthesis of homologous series of larger oligomers. In comparisons, attention needs to be paid whether

  0947-6539/97/0309-1509 $ 17.50+.50/0

the measurements were performed out of resonance; furthermore, differences in experimental techniques need also to be considered. Measurements by degenerated four-wave mixing (DFWM) and electric field-induced second-harmonic generation (EFISH) tend to give a bigger exponent for the power law (between 3 and 5) than THG data.[19]

Unsubstituted PA showed an exponent for the power law in the range of 2.5, but the critical conjugation length seems to be much longer than in PTAs, with about 120 double bonds.[20] Substituted PAs gave exponents between 2.3 and 4.6 depending on the attached substituents, showing clearly the influence of the electron density distribution on the conjugated backbone.[21] A comparison between PDAs and PTAs would be of interest, but second-order hyperpolarizability data for series of homologous PDA oligomers have not been published to the best of our knowledge. THG studies on polythiophene yielded an exponent of 2.8 for the power law.[22] For the critical conjugation length, different, contradicting results have been published, and comparisons to PTAs are therefore difficult. THG measurements disclosed an exponent of 2.4 for poly(3-ethylthiophene ethynylene) and a critical conjugation length of about 10 monomer units (30 double and triple bonds).[23] Thus, the second-order hyperpolarizability γ of different linearly conjugated polymers seems to scale with a power law $\gamma \approx n^a$, with an exponent a around 2.5 for THG measurements. This is significantly below the theoretical predictions and quantum chemical calculations.

THG measurements in the series of tetraethynylethene oligomers were limited to the shorter members **1a–c**, owing to low solubility (Table 3). The existence of additional conjugation paths in these compounds increased the second-order hyperpolarizabilities by about one order of magnitude, as compared to **4a–c**.

Conclusions

A readily available, new series of monodisperse poly(triacetylene) (PTAs) oligomers **4a–f**, ranging from monomer to hexamer, exhibited amazing environmental stability and solubility, which allowed systematic investigation of their physical properties by different methods. In the cyclic voltammetry studies, all six oligomers underwent a reversible one-electron transfer reduction, becoming increasingly facilitated with increasing length of the conjugated backbone, but could not be oxidized below +1.23 V vs. Fc/Fc^+. Whereas a linear fit was obtained in the plot of the first reduction potential against $1/n$ (n = number of monomeric units) in the oligomeric series **4a–f**, the linear correlation vanished upon inclusion of the longer-chain polymers, and an estimation of the effective conjugation length from the electrochemical data therefore was not straightforward.

In the UV/Vis spectra of oligomers **4a–f**, the longest-wavelength absorptions λ_{max} as well as the end absorptions were increasingly bathochromically shifted with increasing conjugation length. From the linear optical properties, the effective conjugation length in PTAs was estimated by various evaluation methods to be in the range of 7–10 monomer units.

Third harmonic generation measurements in the series **4a–f** showed for the second-order hyperpolarizability γ a power law dependence $\gamma \approx n^a$ with a fitted exponent $a = 2.5 \pm 0.1$. This exponent showed an amazing coincidence with that of other conjugated polymers, measured by the same technique in their transparency range. The effective conjugation length for the second-order hyperpolarizability γ was found to be around 10 monomer units. Thus, linear and nonlinear optical methods showed a striking accordance of the effective conjugation length in PTAs. However, it is not well understood at the moment, whether both methods should lead to the same critical conjugation length or not. This will be the subject of further investigations.

The preparation of even larger, monodisperse PTA oligomers is now being pursued in our laboratory in order to close the interesting gap between oligomer and polymer analysis. Once this has been achieved, a reinvestigation of the effective conjugation length by electrochemical methods is also planned.

Experimental Section

General Methods: Reagents and solvents were purchased at reagent-grade from Aldrich or Fluka and used without further purification. Compounds **5** and **6** were prepared as described in refs. [5,9]. Melting points were determined on a Büchi SMP-20 apparatus and are uncorrected. UV/Vis spectra were recorded on a Varian-Cary-5 spectrophotometer at RT, and low-temperature measurements were obtained on a Kontron Uvikon 941 instrument with a home-built cryostat. IR spectra were recorded on a Perkin-Elmer-1600-FT-IR spectrometer. Fluorescence spectra were obtained on a SPEX-1580 double spectrophotometer at RT. ^1H NMR spectra were recorded on a Bruker-AMX-500 instrument, and ^{13}C NMR spectra on a Bruker-AMX-500 (125 MHz) spectrometer with complete proton decoupling. Laser-desorption time-of-flight (LD-TOF) mass spectra were obtained using a Bruker Reflex instrument with an N_2 laser system (337 nm) to desorb and ionize analyte molecules, which were previously dissolved in CH_2Cl_2 and deposited onto the center of the probe tip, and dried under vacuum. All reported data were acquired using the linear positive-ion mode at +15 and 20 kV, respectively. Elemental analyses were carried out by the Mikrolabor in the Laboratorium für Organische Chemie at ETH Zürich.

Third-harmonic generation measurements: Chloroform solutions with initial concentrations of 0.5–1.5 wt% were prepared and later diluted to four lower concentrations. The laser source was a pulsed Nd:YAG laser ($\lambda = 1.064$ μm, 10 Hz repetition rate, pulse duration of 5 ns), which was used to pump an H_2-gas Raman cell yielding a frequency-shifted wavelength of $\lambda = 1.907$ μm. The *s*-polarized beam was then focused onto the sample with an $f = 500$ mm lens. Third-harmonic generation measurements were performed by rotating the 1 mm-thick fused silica cuvette with the solution parallel to the polarization to generate well-known Maker-fringe interference patterns. The Maker-fringe patterns were analyzed in a manner similar to that described in the literature.[24] All measurements were calibrated against fused silica $\chi^{(3)}_{fs} = 3.9 \times 10^{-22}\ m^2\ V^{-2}$ (2.8×10^{-14} esu).[25] A comparison of measurements of fused silica in vacuum and air allowed all subsequent measurements of our solutions to be performed in air.

Synthesis of Oligomers 4b–f: To a solution of **5** (0.087 g, 0.24 mmol, 1 equiv) and **6** (0.210 g, 0.48 mmol, 2 equiv) in dry CH_2Cl_2 (10 mL, molecular sieves 4 Å) was added TMEDA (0.079 g, 0.10 mL, 0.68 mmol) and CuCl (0.019 g, 0.19 mmol) at RT. After the mixture had been stirred under ambient atmosphere for 2 h, an EDTA solution (EDTA = ethylendiaminetetraacetic acid, pH 8) was added and the reaction mixture extracted with CH_2Cl_2 until the washings were colorless. The organic phase was washed with saturated aqeous NaCl solution and dried (anh. $MgSO_4$). Concentration at water aspirator pressure, size-exclusion chromatography (Bio-Rad Bio-Beads S-X1 beads, CH_2Cl_2), flash chromatography (Fluka 40-63 μm (230–400 mesh) SiO_2 60, hexane/PhMe 1:1), and precipitation from MeOH gave the pure oligomers **4b–f** as yellow solids.

(*E*,*E*)-1,12-Bis(trimethylsilyl)-3,4,9,10-tetrakis{[(*tert*-butyl)dimethylsilyloxy]-methyl}dodeca-3,9-diene-1,5,7,11-tetrayne (4b): Yield: 58% (121 mg); M.p.

0947-6539/97/0309-1510 $ 17.50+.50/0 *Chem. Eur. J.* **1997**, *3*, No. 9

97 °C; ^{1}H NMR (500 MHz, $CDCl_3$): δ = 0.075 (*s*, 12H), 0.078 (*s*, 12H), 0.18 (*s*, 18H), 0.892 (*s*, 18H), 0.894 (*s*, 18H), 4.39 (*s*, 4H), 4.45 (*s*, 4H); ^{13}C NMR (125 MHz, $CDCl_3$): δ = −5.21, −5.18, −0.26, 18.34, 18.36, 25.87, 63.81, 63.87, 81.93, 85.41, 101.48, 109.23, 129.59, 133.11; FT-IR ($CHCl_3$): $\tilde{\nu}$ = 2144 (w = weak), 1600 (w) cm^{-1}; UV/Vis ($CHCl_3$): λ = 274 (17600), 286 (19200), 300 (21800), 319 (21400), 351 (28000), 376 (24700); LD-TOF-MS: *m/z*: 870 $[M]^+$, 814 $[M - C(CH_3)_3]^+$; $C_{46}H_{86}O_4Si_6$ (871.71): calcd C 63.38, H 9.94; found: C 63.49, H 9.90.

(*E,E,E*)-1,18-Bis(trimethylsilyl)-3,4,9,10,15,16-hexakis{[(*tert*-butyl)dimethylsilyloxy]methyl}octadeca-3,9,15-triene-1,5,7,11,13,17-hexayne (4c). Yield: 20% (59 mg); M.p. 138 °C; ^{1}H NMR (500 MHz, $CDCl_3$): δ = 0.076–0.082 (*m*, 36H), 0.19 (*s*, 18H), 0.89 (*s*, 54H), 4.39 (*s*, 4H), 4.44 (*s*, 4H), 4.45 (*s*, 4H); ^{13}C NMR (125 MHz, $CDCl_3$): δ = −5.20, −5.18, −0.27, 18.32, 18.34, 18.36, 25.84, 25.86, 63.79, 63.85, 63.87, 81.88, 83.18, 85.22, 87.35, 101.44, 109.51, 129.44, 132.15, 133.45; FT-IR ($CHCl_3$): $\tilde{\nu}$ = 2144 (w), 1600 (w) cm^{-1}; UV/Vis ($CHCl_3$): λ = 271 (26000, sh), 285 (28400), 302 (25300), 322 (24200), 377 (42200, sh), 389 (46200), 407 (36700, sh); LD-TOF-MS: *m/z*: 1235 $[M]^+$, 1177 $[M - C(CH_3)_3]^+$; $C_{66}H_{120}O_6Si_8$ (1234.37): calcd C 64.22, H 9.80; found: C 64.37, H 9.76.

(*E,E,E,E*)-1,24-Bis(trimethylsilyl)-3,4,9,10,15,16,21,22-octakis{[(*tert*-butyl)-dimethylsilyloxy]methyl}tetracosa-3,9,15,21-tetraene-1,5,7,11,13,17,19,23-octayne (4d). Yield: 9% (34 mg); M.p. 168 °C; ^{1}H NMR (500 MHz, $CDCl_3$): δ = 0.075–0.081 (*m*, 48H), 0.18 (*s*, 18H), 0.89 (*s*, 72H), 4.39 (*s*, 4H), 4.43 (*s*, 8H), 4.45 (*s*, 4H); ^{13}C NMR (125 MHz, $CDCl_3$): δ = −5.18, −5.17, −5.14, −0.24, 18.34, 18.35, 18.37, 18.39, 25.86, 25.89, 63.82, 63.86, 63.88, 63.90, 81.86, 83.13, 83.35, 85.21, 87.17, 87.59, 101.46, 109.60, 129.45, 132.00, 132.53, 133.54; FT-IR ($CHCl_3$): $\tilde{\nu}$ = 2359 (w), 2133 (w) cm^{-1}; UV/Vis ($CHCl_3$): λ = 278 (25800, sh), 287 (27100), 301 (25800), 322 (22200), 380 (39700, sh), 403 (52100), 423 (42500, sh); LD-TOF-MS: *m/z*: 1597 $[M]^+$, 1540 $[M - C(CH_3)_3]^+$; $C_{86}H_{154}O_8Si_{10}$ (1597.04): calcd C 64.68, H 9.72; found: C 64.50, H 9.60.

(*E,E,E,E,E*)-1,30-Bis(trimethylsilyl)-3,4,9,10,15,16,21,22,27,28-decakis{[(*tert*-butyl)dimethylsilyloxy]methyl}triaconta-3,9,15,21,27-pentaene-1,5,7,11,13,17,19,23,25,29-decayne (4e). Yield: 2% (9 mg); M.p. 189 °C; ^{1}H NMR (500 MHz, $CDCl_3$): δ = 0.083–0.089 (*m*, 60H), 0.19 (*s*, 18H), 0.90 (*s*, 90H), 4.40 (*s*, 4H), 4.44 (*s*, 12H), 4.46 (*s*, 4H); ^{13}C NMR (125 MHz, $CDCl_3$): δ = −5.20, −5.17, −0.27, 18.32, 18.34, 18.36, 25.83, 25.86, 63.79, 63.82, 63.84, 63.87, 81.81, 83.04, 83.24, 83.35, 85.17, 87.09, 87.35, 87.61, 101.42, 109.59, 129.41, 131.94, 132.32, 132.57, 133.53; FT-IR ($CHCl_3$): $\tilde{\nu}$ = 2359 (w), 2133 (w), 1600 cm^{-1} (w); UV/Vis ($CHCl_3$): λ = 285 (27700), 302 (27100), 321 (23800), 341 (22000, sh), 416 (57200); LD-TOF-MS: *m/z*: 1960 $[M]^+$, 1901 $[M - C(CH_3)_3]^+$; $C_{106}H_{188}O_{10}Si_{12}$ (1959.70): calcd C 64.97, H 9.67; found: C 64.84, H 9.72.

(*E,E,E,E,E,E*)-1,36-Bis(trimethylsilyl)-3,4,9,10,15,16,21,22,27,28,33,34-dodecakis{[(*tert*-butyl)dimethylsilyloxy]methyl}hexatriaconta-3,9,15,21,27,33-hexaene-1,5,7,11,13,17,19,23,25,29,31,35-dodecayne (4f). Yield: 1% (6 mg); M.p. 196 °C; ^{1}H NMR (500 MHz, $CDCl_3$): δ = 0.079-0.086 (*m*, 72H), 0.19 (*s*, 18H), 0.90 (*s*, 108H), 4.40 (*s*, 4H), 4.44 (*s*, 16H), 4.46 (*s*, 4H); ^{13}C NMR (125 MHz, $CDCl_3$): δ = −5.20, −5.18, −0.28, 18.30, 18.33, 18.35, 25.83, 25.86, 63.79, 63.82, 63.85, 63.88, 81.82, 83.04, 83.20, 83.30, 83.38, 85.16, 87.07, 87.29, 87.39, 87.61, 101.45, 109.57, 129.43, 131.94, 132.29, 132.40, 132.59, 133.54; FT-IR ($CHCl_3$): $\tilde{\nu}$ = 2161 (w), 2125 (w), 1678 (w), 1606 (w) cm^{-1}; UV/Vis ($CHCl_3$): λ = 285 (29400), 301 (28400), 321 (26200), 425 (64000); LD-TOF-MS: *m/z*: 2320 $[M]^+$, 2260 $[M - C(CH_3)_3]^+$; $C_{126}H_{222}O_{12}Si_{14}$ (2322.36): calcd C 65.17, H 9.64; found: C 65.07, H 9.65.

X-ray Crystallography:[26] **4a** ($C_{26}H_{52}O_2Si_4$, M_r = 509.05): Single crystals were grown from hexane by slow evaporation at 20 °C; monoclinic space group $P2_1/n$, ρ_{calcd} = 0.962 g cm^{-3}, Z = 2; a = 6.278(8), b = 11.867(14), c = 23.58(4) Å, β = 91.40(12)°, V = 1756(4) Å^3, Syntex P21 diffractometer, $Mo_{K\alpha}$ (λ = 0.71073 Å) radiation, $2\theta \leq 40°$, 1963 unique reflections. The structure was solved by direct methods and refined by full-matrix least-squares analysis (SHELXTL PLUS; heavy atoms anisotropic, H atoms fixed, whereby H positions are based on stereochemical considerations), yielding $R(F)$ = 0.0557, $R_w(F)$ = 0.0780 for 169 variables and 878 independent reflections with $F > 4.0\sigma(F)$.

5 ($C_{20}H_{36}O_2Si_2$, M_r = 364.68): Single crystals were grown from hexane by slow evaporation at 20 °C: monoclinic space group $C2/c$, ρ_{calcd} = 1.004 g cm^{-3}, Z = 4; a = 26.81(2), b = 6.292(5), c = 14.576(13) Å, β = 100.97(7)°, V = 2414(4) Å^3, Syntex P21 diffractometer, $Mo_{K\alpha}$ (λ = 0.71073 Å) radiation, $2\theta \leq 40°$, 1317 unique reflections. The structure was solved by direct methods and refined by full-matrix least-squares analysis (SHELXTL PLUS; heavy atoms anisotropic, H atoms fixed, whereby H positions are based on stereochemical considerations), yielding $R(F)$ = 0.0384, $R_w(F)$ = 0.0551 for 123 variables and 844 independent reflections with $F > 4.0\sigma(F)$.

Acknowledgments: This work was supported by a grant from the ETH Research Council. We thank Andy Taton for assistance in recording low-temperature UV/Vis spectra.

Received: March 25, 1997 [F651]

[1] a) *Electronic Properties of Conjugated Polymers III: Basic Models and Applications* (Eds: H. Kuzmani, M. Mehring, S. Roth), Springer, Berlin **1989**; b) J. S. Miller, *Adv. Mater.* **1993**, *5*, 671–676; c) *Handbook of Conducting Polymers* (Ed: T. A. Skotheim), Dekker, New York **1986**, Vols. 1,2; d) *Conjugated Polymers and Related Materials. The Interconnection of Chemical and Electronic Structure* (Eds: W. R. Salaneck, I. Lundström, B. Ränby), Oxford University Press, Oxford **1993**; e) M. Liphardt, A. Goonesekera, B. E. Jones, S. Ducharme, J. M. Takacs, L. Zhang, *Science (Washington, D. C.)* **1994**, *263*, 367–369; f) N. C. Greenham, S. C. Moratti, D. D. C. Bradley, R. H. Friend, A. B. Holmes, *Nature* **1993**, *365*, 628–630; g) A. Buckley, *Adv. Mater.* **1992**, *4*, 153–158; h) H. S. Nalwa, *Adv. Mater.* **1993**, *5*, 341–358.

[2] a) D. L. Pearson, J. S. Schumm, J. M. Tour, *Macromolecules* **1994**, *27*, 2348–2350; b) P. Seta, E. Bienvenue, *Mol. Electron. Mol. Electron. Devices* **1994**, *3*, 59–78; c) L. Jones II, D. L. Pearson, J. S. Schumm, J. M. Tour, *Pure Appl. Chem.* **1996**, *68*, 145–148; d) J. M. Tour, *Chem. Rev.* **1996**, *96*, 537–553; e) M. D. Ward, *Chem. Ind. (London)* **1996**, *15*, 568–573; f) T. Bartik, B. Bartik, M. Brady, R. Dembinski, J. A. Gladysz, *Angew. Chem.* **1996**, *108*, 467–469; *Angew. Chem. Int. Ed. Engl.* **1996**, *35*, 414–417; g) J. S. Schumm, D. L. Pearson, J. M. Tour, *ibid.* **1994**, *106*, 1445–1448 and **1994**, *33*, 1360–1363; h) R. H. Grubbs, D. Kratz, *Chem. Ber.* **1993**, *126*, 149–157.

[3] a) U. Scherf, K. Müllen, *Synthesis* **1992**, 23–38; b) K. Müllen, *Pure Appl. Chem.* **1993**, *65*, 89–96; c) R. Schenk, H. Gregorius, K. Meerholz, J. Heinze, K. Müllen, *J. Am. Chem. Soc.* **1991**, *113*, 2634–2647; d) J. M. Tour, R. Wu, *Macromolecules* **1992**, *25*, 1901–1907; f) J. Roncali, *Chem. Rev.* **1992**, *92*, 711–738.

[4] a) S. A. Jenekhe, *Macromolecules* **1990**, *23*, 2848–2854; b) J. Grimme, M. Kreyenschmidt, F. Uckert, K. Müllen, U. Scherf, *Adv. Mater.* **1995**, *7*, 292–295; c) J. L. Brédas, R. Silbey, D. S. Boudreaux, R. R. Chance, *J. Am. Chem. Soc.* **1983**, *105*, 6555–6559; d) J. Guay, P. Kasai, A. Diaz, R. Wu, J. M. Tour, L. H. Dao, *Chem. Mater.* **1992**, *4*, 1097–1105.

[5] M. Schreiber, J. Anthony, F. Diederich, M. E. Spahr, R. Nesper, M. Hubrich, F. Bommeli, L. Degiorgi, P. Wachter, P. Kaatz, C. Bosshard, P. Günter, M. Colussi, U. W. Suter, C. Boudon, J.-P. Gisselbrecht, M. Gross, *Adv. Mater.* **1994**, *6*, 786–790.

[6] M. Schreiber, R. R. Tykwinski, F. Diederich, R. Spreiter, U. Gubler, C. Bosshard, I. Poberaj, P. Günter, C. Boudon, J.-P. Gisselbrecht, M. Gross, U. Jonas, H. Ringsdorf, *Adv. Mater.* **1997**, *9*, 339–343.

[7] a) J. Anthony, C. Boudon, F. Diederich, J.-P. Gisselbrecht, V. Gramlich, M. Gross, M. Hobi, P. Seiler, *Angew. Chem.* **1994**, *106*, 794–798; *Angew. Chem. Int. Ed. Engl.* **1994**, *33*, 763–766; b) J. Anthony, A. M. Boldi, Y. Rubin, M. Hobi, V. Gramlich, C. B. Knobler, P. Seiler, F. Diederich, *Helv. Chim. Acta* **1995**, *78*, 13–45.

[8] C. Boudon, J. P. Gisselbrecht, M. Gross, J. Anthony, A. M. Boldi, R. Faust, T. Lange, D. Philp, J.-D. Van Loon, F. Diederich, *J. Electroanal. Chem.* **1995**, *394*, 187–197.

[9] a) R. R. Tykwinski, M. Schreiber, R. Pérez Carlón, F. Diederich, V. Gramlich, *Helv. Chim. Acta* **1996**, *79*, 2249–2281; b) J. Anthony, Ph.D. Thesis, University of California, Los Angeles, **1993**.

[10] R. Giesa, R. C. Schulz, *Polym. Inter.* **1994**, *33*, 43–60.

[11] CVFF force field, Insight II, Version 95.0, Biosym Technologies, San Diego 1995.

[12] The maximum of the longest-wavelength absorption λ_{max} was obtained by deconvolution for **3a** and **3b** as 480 ± 1 nm (E_{max} = 2.58 eV).

[13] The solution optical band gap was estimated by the intersection of the *x* axis and the tangent passing through the turning point of the lowest-energy absorption band.

[14] The solution optical band gap for **3a** is 2.40 eV. See also ref. [5].

[15] G. Wenz, M. A. Müller, M. Schmidt, G. Wegner, *Macromolecules* **1984**, *17*, 837–850.

[16] a) H. Kuhn, *Fortschr. Chem. Org. Naturst.* **1958**, *16*, 169–205; b) H. Kuhn, *ibid.* **1959**, *17*, 404–451.

[17] C. Bosshard, R. Spreiter, P. Günter, R. R. Tykwinski, M. Schreiber, F. Diederich, *Adv. Mater.* **1996**, *8*, 231–234.

[18] a) K. C. Rustagi, J. Ducuing, *Opt. Commun.* **1974**, *10*, 258–261; b) G. P. Agrawal, C. Cojan, C. Flytzanis, *Phys. Rev. B* **1978**, *17*, 776–789; c) J. R. Heflin, K. Y. Wong, O. Zamani-Kamiri, A. F. Garito, *ibid.* **1988**, *38*, 1573–1576; d) C. P. DeMelo, R. Silbey, *J. Chem. Phys.* **1988**, *88*, 2558–2566.

[19] a) G. S. W. Craig, R. E. Cohen, R. R. Schrock, R. J. Silbey, G. Puccetti, I. Ledoux, J. Zyss, *J. Am. Chem. Soc.* **1993**, *115*, 860–867; b) M.-T. Zhao, B. P. Singh, P. N. Prasad, *J. Chem. Phys.* **1988**, *89*, 5535–5541; c) H. Thienpont, G. L. J. A. Rikken, E. W. Meijer, W. ten Hoeve, H. Wynberg, *Phys. Rev. Lett.* **1990**, *65*, 2141–2144.

[20] I. D. W. Samuel, I. Ledoux, C. Dhenaut, J. Zyss, H. H. Fox, R. R. Schrock, R. J. Silbey, *Science (Washington, D. C.)* **1994**, *265*, 1070–1072.

[21] J. Zyss, *Molecular Nonlinear Optics: Materials, Physics and Devices*, Academic Press, Boston **1993**.

[22] L.-T. Cheng, J. M. Tour, R. Wu, P. V. Bedworth, *Nonlinear Optics* **1993**, *6*, 87–92.

[23] I. D. W. Samuel, I. Ledoux, C. Delporte, D. L. Pearson, J. M. Tour, *Chem. Mater.* **1996**, *8*, 819–821.

[24] F. Kajzar, J. Messier, *Phys. Rev. A* **1985**, *32*, 2352–2363.

[25] B. Buchalter, G. R. Meredith, *Appl. Opt.* **1982**, *21*, 3221–3224.

[26] Crystallographic data (excluding structure factors) for the structures reported in this paper have been deposited with the Cambridge Crystallographic Data Centre as supplementary publication no. CCDC-100298. Copies of the data can be obtained free of charge on application to The Director, CCDC, 12 Union Road, Cambridge CB21EZ, UK (Fax: Int. Code +(1223)336-033; e-mail: deposit@chemcrys.cam.ac.uk).

  0947-6539/97/0309-1512 $ 17.50+.50/0